Interpretable Tracking and Detection of Unstable Approaches Using Tunnel Gaussian Process

Sim Kuan Goh, Senior Member, IEEE
School of Electrical Engineering and Artificial Intelligence, Xiamen University, Malaysia.

Narendra Pratap Singh
Airports Authority of India, Lucknow Airport, India.

Zhi Jun Lim, Sameer Alam
Air Traffic Management Research Institute, Nanyang Technological University, Singapore.

***Abstract*— Approach and landing are phases of flight with the highest accident risk. Advanced instruments and procedures have been developed to provide precise navigation for a stabilized approach and landing. With the proliferation of sensing techniques, real-time 4D trajectories can be captured at higher spatial-temporal resolution and enable data-driven decision-making for air traffic controllers (ATCO). This research attempts to augment the existing rule-based stable approach criteria using data-driven and interpretable tunnel Gaussian process (TGP) models to probabilistically characterize the 4D approach and landing parameters. The TGP explicitly and continuously models the underlying distribution of approach and landing parameters and their interrelations. In addition, it provides a comprehensible probabilistic description of anomalies in approach and landing parameters. Based on the trained TGP, we infer the landing parameters of go-around tracks recorded by the advanced surface movement guidance and control system (A-SMGCS) and analyze their adherence to stabilized approach criteria. Empirical results show that anomalous scores were in line with the factors (as reported to ATCOs) in all go-around data in the test dataset, between 0.5 NM (missed approach point) to 7.6 NM from the touchdown threshold, and provides better probabilistic insights of non-compliance, comparing to existing work. Hence, the proposed TGP can provide a ground-based safety net for the compliance of stable approaches. Furthermore, the proposed TGP-based anomaly tracking methods can be directly applied to other types of landing systems (e.g., GNSS landing system and RNAV approaches).**

***Index Terms*—Tunnel Gaussian Process, Unstable Approaches, Data-Driven Air Traffic, Flight Safety**

This research is supported by the National Research Foundation, Singapore, and the Civil Aviation Authority of Singapore, under the Aviation Transformation Programme. Any opinions, findings and conclusions or recommendations expressed in this material are those of the author(s) and do not reflect the views of National Research Foundation, Singapore and the Civil Aviation Authority of Singapore. The first author acknowledges the support from Xiamen University Malaysia Research Fund (XMUMRF/2022-C10/IECE/0039). *(Corresponding authors: S. K. Goh and S. Alam.)*

Sim Kuan Goh is with the School of Electrical Engineering and Artificial Intelligence, Xiamen University, Malaysia (e-mail: simkuangoh@gmail.com). Narendra Pratap Singh is with the Airports Authority of India, Lucknow Airport, India (e-mail: naren.p.singh@gmail.com). Zhi Jun Lim and Sameer Alam are with the Air Traffic Management Research Institute, Nanyang Technological University, Singapore (e-mail: zhijun001@e.ntu.edu.sg, sameeralam@ntu.edu.sg).

Supplementary materials include additional analyses and figures.

Color versions of one or more of the figures in this article are available online at http://ieeexplore.ieee.org.

I. INTRODUCTION

Approach and landing remain to be the most perilous events in aircraft operations. To circumvent the risks, there are a number of pre-established criteria to be met for a safe landing, including aircraft configuration, attitude, airspeed, power/thrust settings as well as runway alignment (touch down point). During the approach and landing phases, all such aircraft configuration parameters must be within specified limits in order to execute a stable approach and successful landing. If an aircraft executes a landing in an unstable configuration, it may result in a long or short landing by missing the touchdown zone, or touching down too fast, too hard, off the runway centerline, and in the incorrect attitude [1]. These may, in turn, lead to a "bounced" or hard landing or a runway excursion incident leading to structural damage to aircraft and, at times, can be fatal too [2].

As per the Boeing safety report (2007-2016) on worldwide commercial jet airplane accidents, fatal accidents, and on-board fatalities by the phase of flight, it has been observed that the final approach and landing constituted 48% of total fatal accidents and on-board fatalities [3]. In the majority of these accidents, "unstable approaches" were identified as a direct or indirect factor. The international air transport association (IATA), an airline regulatory body, identified an "unstable approach" and associated failure to perform a "go-around" as the single most important factor in runway excursions in a safety report on runway excursions (2004-2009) [4]. There can be many factors that may contribute to an unstable approach. This can include external factors (weather, tailwind), human factors (fatigue, workload, poor planning, pilot error, ATCO interaction), and operational factors (arrival procedures, approach/STAR design, etc.) [5]. Moreover, airlines have their own standard operating procedures (SOPs) to determine the stabilized approach configuration, which includes parameters ranges specific to each aircraft type, such as landing gear, wing flaps, speed brakes, speed and thrust, including vertical speed limitations and acceptable vertical and lateral displacement from the typical approach path. IATA also has a set of recommended standards for a stabilized approach that specify a minimum height at which an aircraft stabilization in visual and instrumental meteorological conditions must be achieved [6].

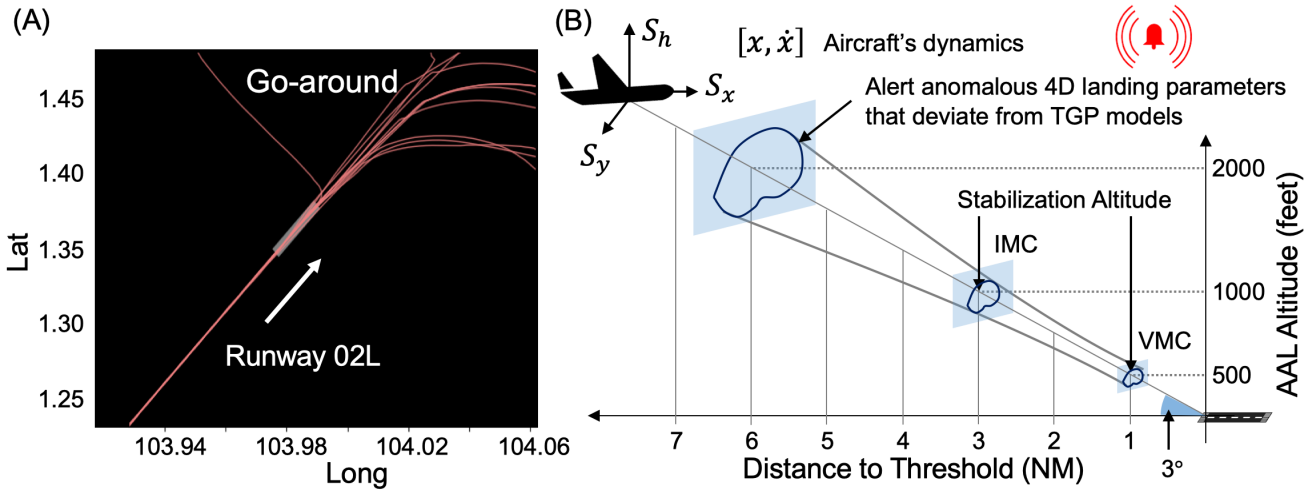

Fig. 1: Panel (A) shows the trajectories of go-around cases recorded by A-SMGCS. Panel (B) illustrates instrument navigation guidance for approach and landing.

Airline industry data reveals an average of $1,000$ approaches per day being conducted while the aircraft is in an unstable configuration. However, most pilots continue with the approach and make the landing. Only 3% of such flights aborted the landing and executed go-around [7]. This may also result from the flight crew being under pressure to continue approaches to reduce delays, fatigue, and peer pressure. Although it remains the responsibility of the pilot in command (PIC) to decide not to continue an approach if, in his or her opinion, the approach is becoming unstable, ATCOs can play a role in the chain of events that leads to an unstable approach [8]. Though ATCOs are not required to watch the approaching aircraft and detect any flight path deviations during the final approach at the expense of their other tasks, there is no explicit rule that restricts an ATCO from determining if a flight deviation should be considered critical to advise PIC a go-around procedure. ATCO may only rely on his common sense and experience, but an appropriate reaction could significantly reduce the seriousness of an incident.

Therefore, it would be prudent to design automation aids and complementary tools [9], [10], [11] so that ATCOs can better respond when they detect a flight path deviation and, therefore, suggest another effective course of action to avoid serious incidents and accidents, illustrated in Fig. 1. They may also help ATCOs be prepared for a go-around and avoid unnecessary changes to the missed approach procedure, and instruct a go-around if safety consideration requires it. Such aids usually enhance the situational awareness of controllers by providing alerts/warnings of the contributing factors to – and risks associated with – unstabilized approaches. Moreover, since an unstable approach and go-around can perturb the arrival schedules and landing slots, in addition to the negative impacts on safety, an early detection, diagnosis, and prognosis of an unstable approach can facilitate corrective actions, and/or rescheduling, re-routing ahead of time. Landing aids have also been studied and developed for unmanned aerial vehicles [12].

In this paper, we attempt to augment the existing rule-based stable approach criteria using data-driven and interpretable tunnel Gaussian process (TGP) models that probabilistically characterize the 4D approach and landing parameters for unstable approaches tracking and detection. The main contributions of this paper include:

- Investigate the use of TGP, developed in authors' recent work [13], for gaining continuous and probabilistic insights into approach and landing parameters and their interrelations.
- Assessment of the practical use of TGP as a comprehensible ground-based safety net for the compliance of stable approaches using operational data.
- Comparative analysis of TGP with an existing method that learned the probabilistic description of approach and landing parameters.

II. BACKGROUND

Recently, advances in sensing techniques and machine learning algorithms have paved the way for data-driven decision-making for safety-critical engineering applications [14], [15]. The categorization of approach and landing parameters into stabilized or unstable approaches can be formulated as a binary classification problem or an anomaly detection problem, which can be solved using supervised and unsupervised learning models [16]. With the availability of labeled data, supervised learning models can be formulated for unstable approach detection. However, data labeling is a time-consuming process for subject matter experts, and anomalous data can hardly be characterized fully. Moreover, anomalous data is usually underrepresented and causes an imbalanced data problem [17]. In contrast, unsupervised learning models extract the underlying features and representations from

unlabeled data. Popular unsupervised learning methods for anomaly detection include negative selection algorithms [18], one-class classifiers [19], autoencoder methods [20] and density-based approaches [21]. This research focuses on density-based approaches that characterize the underlying probabilistic distributions of unlabeled approach and landing parameters.

Machine learning and data-driven models have been adopted to study aircraft approach landing phases such as go-around prediction [22], unstable approach detection [23], [24], prediction [25], landing metrics [26], landing anomaly [27], and landing slot allocation [28], [29]. While these works provide statistical, detective, and predictive models for landing analysis, a few pioneering studies developed data-driven approaches and investigated approach procedures. Prominent amongst them use generative models, such as Gaussian mixture model [30] and Gaussian process (GP) model [31], to generate new trajectories based on the probabilistic description of historical trajectories. In contrast to non-generative methods based on physical equations of motion [32], [33], trajectory clustering methods [34], [35], these methods provide a data-driven approach to assess procedure designs, collision risks and perform anomaly detection. Our work is in line with these works to develop decision-making aids. We attempt to aid approach and landing decisions by providing not only a single anomalous score of stability, but also the details of any non-conformance in landing parameters, which in turn, facilitates necessary corrective actions in real-time and re-planing ahead of time.

Notwithstanding that machine learning has been developed to support decision-making in high-stakes domains (e.g., finance, healthcare, air traffic management) [36], [37], these methods are generally optimized solely for fitting performance, providing little comprehensive and actionable insights [38], [39]. Recent research has contributed to enhancing the interpretability of machine learning models [40]. Machine learning models, with built-in interpretability [41], [42] and properties that can incorporate prior knowledge [43], have demonstrated improved fitting performance. Moreover, interpretability enhances user readability and allows informed decision-making when machine learning is used for advisories [39]. This interpretable information is essential and critical for anomaly detection tasks where diagnosis and corrective actions are required. Our work builds upon these relevant studies, developing an interpretable approach and landing aid for tracking and detecting unstable approaches.

In this paper, we introduce a continuous and interpretable method for 4D tunnel views of aircraft landing parameters and trajectories using tunnel Gaussian process (TGP) models [13]. Two variants of TGP models, which are a hybrid of sparse variational Gaussian process [44] (SVGP) and polar Gaussian process [45], are extended to elucidate the interrelation between approach and landing parameters and detect the anomaly. Using go-around tracks in the advanced surface movement guidance and control system (A-SMGCS) data, we demonstrate that the proposed TGP model can track and explicate the unstable approach parameters with additional benefits (i.e., continuity, consistency, and comprehensibility) compared to existing work. The proposed method can augment existing stabilized approach rules with probabilistic descriptions of adherence to nominal landing parameters and hence provide an additional safety-net for pilots and ATCOs.

This paper is organized as follows: Section III describes the proposed methodology and framework. In Section IV, the experimental design that includes the A-SMGCS data processing pipeline and TGP analysis are outlined, followed by results and discussion in Section V, and finally, the conclusion is presented in Section VI.

III. METHODOLOGY

In this section, we describe the problem of probabilistic 4D trajectory learning using approach and landing parameters and the proposed framework for tracking and detecting unstable approach parameters using two variants of TGP models. The dataset used here is then described. Subsequently, the main components in the TGP framework are introduced and the applications of TGP for tracking and detecting anomalous landing parameters are demonstrated.

A. Problem Formulation

Decision on the continuation of an approach to land depends on a set of stabilized approach criteria on approach and landing parameters. The criteria need to be continuously and consciously observed and managed to reduce approach and landing risks. This research aims to augment the existing rule-based stable approach criteria using data-driven methods and investigate the use of interpretable TGP models to probabilistically characterize the 4D approach and landing parameters.

Specifically, TGP is utilized to model aircraft dynamics during a precision runway approach (an approach procedure supported by vertical and lateral guidance signals generated by a ground-based Instrument Landing System (ILS)), given 4D approach and landing trajectories. In [23], GP models were used to develop probabilistic bounds on lateral, vertical, speed, and track angle profiles for anomaly analysis and detection in Cartesian coordinates (C_x, C_y, C_l), illustrated in Fig 3. We took a step forward from side view analysis to 4D tunnel analysis using TGP [13] in cylindrical coordinates (ρ, θ, l) where (ρ, θ) is polar coordinate defined on the longitudinal axis along the pole l in cylindrical coordinates, ρ is the distance from the pole and θ is a clockwise angle from C_y. θ also denotes TGP bearing here. Cylindrical representations allow explicit modeling of aircraft's trajectory envelop (also known as trajectory dispersion), which is a 2-dimensional manifold that lies in a 3-dimensional space. Hence, it is apt for 4D trajectories that follow specific paths (i.e., instrumental landing). Here, cylindrical representation facilitates the explicit character-

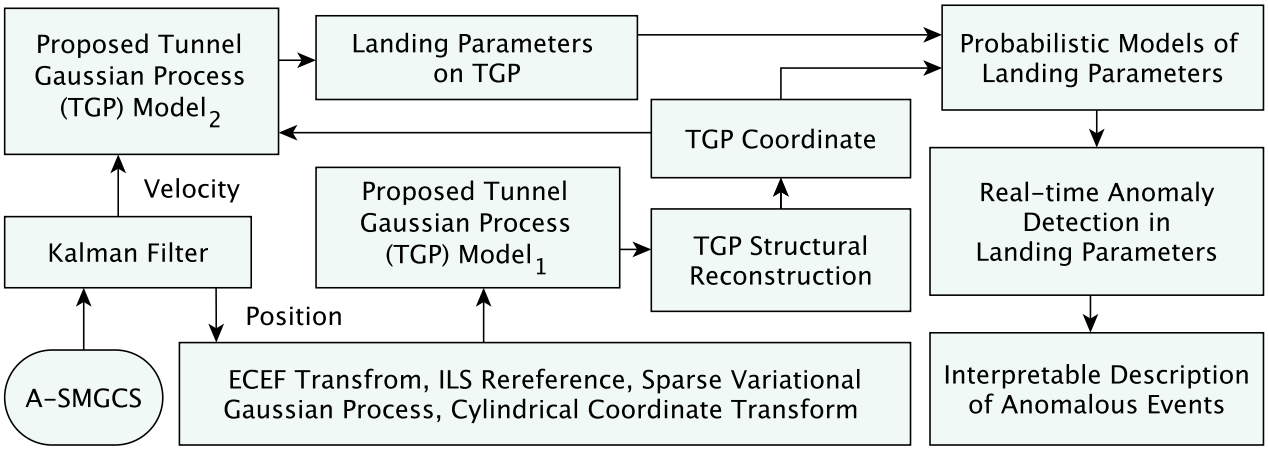

Fig. 2: Proposed TGP framework for tracking and explicating unstable approach parameters.

ization of the probabilistic structure of the approach and landing trajectories. Building on top of TGP models, we extend it for tracking and detection of unstable approach parameters.

B. Proposed Framework

The overall architecture of the proposed framework is illustrated in Fig. 2. The framework comprises procedures such as data preparation (that involves Kalman filtering, earth-centered earth-fixed (ECEF) transformation, extraction of localizer and glide path deviation, normalization), estimation of the non-linear pole in cylindrical coordinate, cylindrical coordinate transformation and training of two TGP models. Subsequently, the proposed TGP models are applied to approach and landing data.

C. A-SMGCS Data

A-SMGCS [46], is a ground-based surveillance system that is used for routing and guidance of the aircraft during ground movement operations (especially in low visibility conditions). Although A-SMGCS is mainly used for surface movement operations, it can also record and track aircraft trajectories in the vicinity of airports, especially when the aircraft is aligned on the final approach path (around 5nm-7nm) from the runway threshold.

The A-SMGCS tracks consist of all arrivals and departures along with other surface vehicles at airports. The recorded data comprehends the aircraft flight tracks and comprises the position of aircraft in latitude and longitude, aircraft identity, reported altitude, and velocity. These tracks are updated and recorded at a rate of 1 sec and complemented by flight plan data. In this study, the focus is on A-SMGCS data related to the landing and approach phase, which includes horizontal positional information – latitude and longitude in UTM WGS84 format, vertical positional information – altitude in feet above mean sea level, ground speed in meters per second and aircraft wake-turbulence category. One month of A-SMGCS data collected from Singapore Changi airport is used for training TGP models, with a total of 2212 medium wake category aircraft and 2305 heavy wake category aircraft. The same dataset as in [23] is used, with pre-processing steps details in [23]. Four months of A-SMGCS go-around tracks are used to assess TGP models.

D. Kalman Filter

Kalman filter (KF), an optimal state observer, has paved the way to address many important real-world engineering problems. Given a model of dynamics and on-board sensor measurements, KF models the states and measurements as follows:

$$\begin{aligned} x_0 &\sim N(\mu_0, \Sigma_0) \\ x_{t+1} &= A_t x_t + b_t + \epsilon^1_{t+1} \\ y_t &= C_t x_t + d_t + \epsilon^2_{t+1} \\ \epsilon^1_t &\sim N(0, Q) \\ \epsilon^2_t &\sim N(0, R) \end{aligned} \tag{1}$$

where x_t is the system state at time t, y_t is the measurement at time t, Q and R are the transition and observation co-variances, A and C are the transition and observation matrices, b_t and d_t are the transition and observation offsets. The parameters of KF can be estimated using the expectation maximization (EM) algorithm [47]. KF is used to estimate the descent rate, which is not available in A-SMGCS, capturing the relationship between the instantaneous descent rate and instantaneous change in height. While KF is used here, the non-linear unscented KF can be utilized given measurement noise and process noise.

1. *ECEF and ILS Deviation*

Earth-centered earth-fixed (ECEF) coordinate system [23], is adopted in this study. In this coordinate

system, the coordinates of trajectories (x, y, z) share the same unit. The ECEF transform is detailed in [23]. Subsequently, the position of an aircraft P on its approach and landing trajectory can be referenced to the configured ILS path and obtained as $(x_{lateral}, x_{glidepath}, l)$.

E. Sparse Variational Gaussian Process

This section describes GP and the sparse variational variant, which form the main components in TGP. The fundamental building blocks GP models the probabilistic mapping function $f(x)$, given $D = (x_i, y_i)_{i=1}^n = (X, Y)$, where X is $(n \times d)$ dimension input with $x_{i\,i=1}^n \in R^d$ and y is output $y_{i\,i=1}^n \in R$, and n is the total number of data instances:

$$y_i = f(x_i) + \epsilon_i \tag{2}$$

where f is modeled using Gaussian process $GP(m_u, K)$ with mean function m_u and co-variance function K and ϵ_i is Gaussian white noise with $N(0, \sigma^2)$.

Given a new data point x_*, the probability distribution of y_* can be obtained as follows:

$$p(y_*|x_*, X, y) = N(\mu_*, \sigma_*^2) \tag{3}$$

where $\mu_* = K_{*n}(K_{nn} + \sigma^2 I)^{-1} y$ and $\sigma_*^2 = K_{**} - K_{*n}(K_{nn} + \sigma^2 I)^{-1} K_{n*} + \sigma^2$. K_{nn} is the co-variance matrix between training data, K_{**} is the co-variance matrix between the new data points, K_{*n} is the co-variance matrix between the new data points and training data, and K_{n*} is the co-variance matrix between the training data and the new data points. Hence, the GP provides prediction μ_* and uncertainty σ_* given x_*. One issue of the basic form of GP is the computational complexities of $O(n^3)$ and storage complexity of $O(n^2)$. The complexities hinder the application of GP to big data.

Sparse Variational Gaussian Process (SVGP) was developed to address the computational and storage complexity of GP models, enabling GP to learn millions of data points [44]. To circumvent the complexity, SVGP combines stochastic variational inference with inducing variables for GP training. SVGP introduces input-output pairs Z, u as inducing variables, where u of the size M that contains values of the function f at the points Z that lie in the same input data space of x. The variable u works as a global variable with a variational distribution $q(u) = \mathcal{N}(u \mid m_u, S)$, a multivariate normal distribution with mean m_u and co-variance S. The training of SVGP is through the optimization of the following variational bound $\mathcal{L}$:

$$\begin{aligned}\mathcal{L} = \sum_{i=1}^{n} \Bigg\{ & log\mathcal{N}(y_i \mid k_i^\top K_{mm}^{-1} m_u, \beta^{-1}) \\ & - \frac{1}{2}\beta \tilde{k}_{i,i} - \frac{1}{2} tr(S\Lambda_i) \Bigg\} \\ & - KL(q(u) \parallel p(u))\end{aligned} \tag{4}$$

where k_i is the i^{th} column of K_{mn} and $\Lambda_i = \beta K_{mm}^{-1} k_i k_i^\top K_{mm}^{-1}$, K_{mm} and K_{mn} are kernel between the inducing points and between the inducing points and training data points, considering independent Gaussian noise of precision β. KL is the abbreviation for Kullback–Leibler divergence. $\tilde{k}_{i,i}$ is the i^{th} diagonal element of $\tilde{K} = K_{nn} - K_{nm} K_{mm}^{-1} K_{mn}$. The derivation and natural gradients to optimize the bound are provided in [44]. SVGP is used to estimate the non-linear pole of the data. Moreover, it will be modified and merged with polar GP to develop TGP.

1. Cylindrical Coordinate Transformation

It is important to ensure that the pole of the cylindrical coordinate passes through the center of trajectories. Based on the observation, 4D trajectories are not straight lines. To address this, the continuous mean in lateral $x_p(l)$ and glide slope $y_p(l)$ deviation of the work [23] by SVGP can be used to model a non-linear pole (x_p, y_p, l).

Subsequently, the coordinate $(C_x, C_y, C_l) = (x_{lateral} - x_p, x_{glideslope} - y_p, l)$, illustrated in Fig. 3, can be transformed to TGP coordinate $T = (\rho, \theta, l)$ defined in Section III-A.

F. Polar Gaussian Process

Polar GP [45] is another important component of TGP models that can be extended to cylindrical coordinates. Polar GP has been motivated by the problems of prediction on circular domains by exploiting the geometry of a disk. It is designed to address two physical processes involving rotation and diffusion from the center of a disk in microelectronics and environmental engineering, where geodesic distance is crucial. A unit disk D can be defined as:

$$D = \{(\rho cos\theta, \rho sin\theta), \rho \in [0, 1], \theta \in [-\pi, \pi]\} \tag{5}$$

where ρ denotes radial coordinate, θ denotes angular coordinate. D can be extended to cylinder C by $[0, 1] \times D$. In [45], two sufficient conditions for the positive definiteness of the kernel are described. C^2 - Wendland function, a compactly supported radial basis function (RBF) on $\mathbb{R}$, guaranteed the kernel on the geodesic distance to be positive definite. The function is as follows:

$$W_c(t) = \left(1 + \tau \frac{t}{c}\right)\left(1 - \frac{t}{c}\right)_+^\tau \tag{6}$$

where t is the geodesic distance, $\{c \in \mathbb{R}, 0 < c \leq \pi\}$ and $\{\tau \in \mathbb{R}, \tau \leq 4\}$. $()_+$ is a rectifier function that is linear to a positive input but zeroes to negative input. For the case of a disk, $c = \pi$.

G. Tunnel Gaussian Process

TGP unified the SVGP and polar GP and addressed a few issues of them [13]. SVGP's paper does not investigate polar and cylindrical coordinates that involve

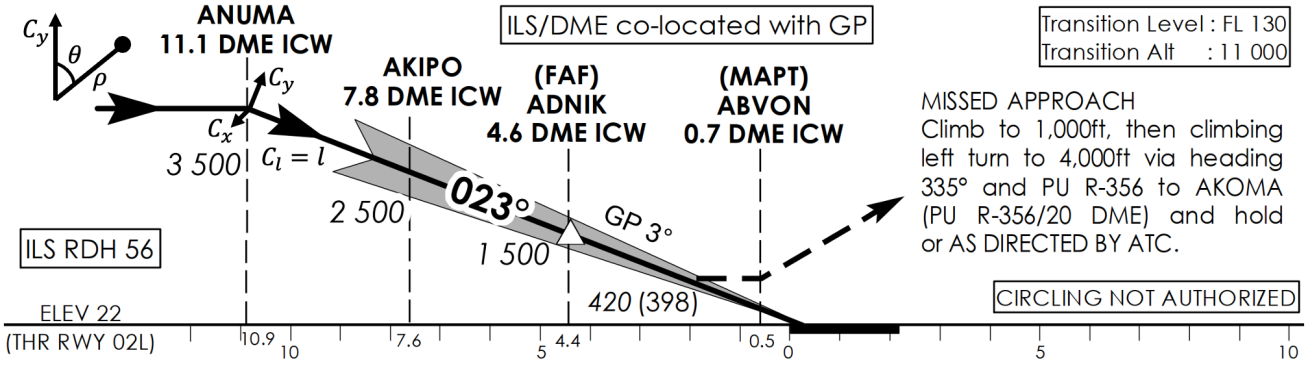

Fig. 3: Illustration of coordinate systems on instrument approach chart (with 2 intermediate fixes ANUMA & AKIPO along with final approach fix ADNIK (FAF), and missed approach point ABVON) for runway 02L, Changi Airport (WSSS), Singapore [Source: AIP, Singapore]. The Cartesian coordinates (C_x, C_y, C_l) and cylindrical coordinates (ρ, θ, l) are illustrated, where C_l and l are identical coordinates. The coordinate system on the top left corner is shown from the perspective of the aircraft flying into the page. It is noteworthy that C_l is learned from 4D approach trajectories and is not required to be a straight line.

geodesic distance. The distance causes the kernel to be non-positive definite. While polar GP works can perform prediction on circular domains, it is not directly applicable to A-SMGCS positional data, which is non-concentric. Besides, it does not address structural reconstruction given the data. Nonetheless, each of them has its own important and unique properties. SVGP enables GP to learn from a big amount of data, while polar GP facilitates GP to handle circular domains.

The equations in SVGP and polar GP were rewritten to develop TGP, detailed in our recent work [13]. The modifications allow TGP to inherit the advantages of both SVGP and polar GP. First, TGP can learn and handle big data in cylindrical coordinates, facilitating the structural reconstruction of 4D trajectories. Second, the kernel functions of polar GP are rewritten to be in a differentiable form, enabling the gradient-based optimization of TGP. Third, the heteroscedasticity of 4D trajectories is taken into account in the Gaussian process framework. Two variants of TGP models were developed. TGP model 1 is a process of two components: angular process $A(\theta)$ and longitudinal process along with the ILS path $L(l)$, while TGP model 2 has an extra radius process $R(\rho)$. The work [13] has demonstrated TGP's capability in reconstructing the 4D tunnel views of approach and landing parameters from historical A-SMGCS data, as shown in supplementary Fig. S1. In [13], the quantitative performance of TGP in comparison with Gaussian mixture models was discussed, where TGP is more robust in capturing the underlying probabilistic distribution of complex trajectories. Moreover, other landing parameters (e.g., velocity) can also be defined on top of the estimated volumic structure. Given the pre-processed data, TGP models 1 processes the position data by combining SVGP (for reducing the computational complexity) and polar GP (for dispersion modeling in cylindrical coordinate). TGP model 2 learns the landing parameters (i.e., velocity) that are defined on TGP model 1. The interactive visualizations are also available at https://simkuangoh.github.io/TunnelGP/.

Based on the predictive probabilistic distribution $N(\mu_*, \sigma_*^2)$ of TGP's structure and parameters estimated on the TGP structure, Z-score can be computed as follows:

$$Z = \frac{x - \mu_*}{\sigma_*} \tag{7}$$

Z-score is the number of standard deviations by which the value of an approach and landing parameter is above or below the mean value of what is being measured. Here, the Z-scores for each approach and landing parameter are analyzed. Given aircraft positional vector P defined in Section III-1, longitudinal speed along the glide slope S_x, lateral speed from the center-line S_y, and descent rate S_h, $Z(P)$ that indicates the anomalous scores of aircraft position and probe $Z(S_x)$, $Z(S_y)$, $Z(S_h)$ for the anomalous scores of longitudinal, lateral speed and descent rate are computed.

The prediction interval of the future observation of approach and landing parameters, given Z-score, can be defined over a range $[l, u]$, as follows:

$$\begin{aligned} \gamma = P(l < X < u) &= P(\frac{l-\mu}{\sigma} < \frac{X-\mu}{\sigma} < \frac{u-\mu}{\sigma}) \\ &= P(\frac{l-\mu}{\sigma} < Z < \frac{u-\mu}{\sigma}) \end{aligned} \tag{8}$$

where μ and σ are defined in Equation 3 and can be obtained from the trained TGP models. The equation provides the probability γ that an approach parameter falls within $[l, u]$. These values can be adjusted flexibly depending on the desired sensitivity and specificity trade-off detecting anomalous approach and landing parameters along the glide slope. It is worth noting that the interval $[l, u]$ and γ can be adjusted without re-training the TGP models.

1. TGP's Hyper-parameters

The number of inducing points M for SVGP is 100, and it is 300 for TGP. The training batch size is 400 for SVGP and 800 for TGP. For speed defined on TGP bounds, M and training batch are selected to be 512 and 1000. These parameters are empirically chosen to achieve the main objective of this work. Higher M and training batch size can always be selected for greater modeling resolution. However, it will also result in higher computational and storage costs. All the other parameters are optimized using Adam optimizer [48].

IV. EXPERIMENTS

This section describes the operational environment, and experiments to elucidate the interrelation between approach and landing parameters and investigate all go-around tracks using TGP models, shown in Fig. 2. Subsequently, we illustrate the anomalous scores of landing parameters and demonstrate how TGP provides an interpretable description of anomalous landing parameters.

A. Operational Environment

Fig. 3 shows the published ILS landing procedure for runway 02L of Singapore Changi airport. As per this ILS chart, an aircraft must align to ILS horizontally while maintaining a track angle of 23° and vertically descending on a glide slope of 3° from a fix ANUMA, which is 11.1 NM from the runway threshold. The permissible horizontal and vertical deviations on ILS are available to the pilots and they monitor the adherence to the ILS. The anonymized go-around tracks and the reported reasons for go-around are provided in Fig. 1 and Table I.

B. Experimental Pipeline

The experimental steps include data preparation, feeding of data into the TGP pipeline, and case studies on go-around tracks using A-SMGCS data.

1. Data Preparation

The pre-processing of A-SMGCS data includes Kalman filtering, ECEF, and ILS re-reference discussion in Section III. Given positional data (x, y, z), it can be represented the data as (C_x, C_y, C_l), where C_l is the longitudinal axis along the pole in the coordinate system.

2. TGP Pipeline

First, the standard scaler is applied to C_x and C_y to normalize them, while the min-max scaler is used for C_l such that it ranges between -1 and 1. Next, SVGP is used to derive the non-linear pole for cylindrical coordinate transformation. After the transformation, the TGP model 1 is trained to model the probabilistic structure of the dense point cloud from 4D trajectories. Subsequently, the other landing parameters (i.e., speeds with respect to ILS, S_x, S_y, S_h for longitudinal speed, lateral speed, and descent rate) are trained using TGP model 2. These two models elucidate the interrelation between landing parameters.

3. Case Studies of Go-around at Singapore Changi Airport

We also evaluate the proposed model's efficacy by tracking and explaining the unstable approach parameters that lead to go-around. All go-around tracks in the dataset for runway 02L at Singapore Changi Airport were studied using proposed TGP models, which can be found in Table I.

As weather and visibility impact approach and landing safety and performance, aviation routine weather reports (METAR) are used in this study. Moreover, TGP findings are compared to the go-around and unstable approach reports. Reasons for go-around for all 14 flights are given in Table I along with anomalies observed by the proposed TGP model. In the experiment, landing parameters, which have an absolute Z-score greater than 2 (equivalent to $2\sigma_*$ away from the μ_*), are labeled to be anomalous events.

4. Comparative Analysis with Existing Work

To establish a baseline for assessing TGP, an existing method by Barratt et al. [30], which is the closest to the current study, is selected. Both works share the same objective of learning probabilistic descriptions of approach and landing parameters. Barratt et al. [30] slightly modified the training procedures of Gaussian mixture models (GMM) for trajectories, referred to as modified GMM (mGMM) here. The details of mGMM and how it can be utilized for tracking and detection of unstable approaches are provided in Section 2 of the Supplementary Materials due to space limitations. Given the probabilistic description of mGMM, landing parameters that have an absolute Z-score greater than 2 (equivalent to two standard deviations away from the mean), are labeled to be anomalous events.

V. RESULTS & DISCUSSION

In this section, we analyze the interrelation between landing parameters by investigating the relationship between ILS deviation and speed using TGP models. The results are shown in Figs. 4-5 and supplementary Figs. S2-S5. Specifically, we investigate the influence of vertical deviation from glide slope ΔGS and lateral deviation from localizer ΔLOC to S_x, S_y, S_h, when the Z-scores in Equation 7 are 1, 2, and 3, which correspond to deviations of $\sigma, 2\sigma, 3\sigma$ in Equation 8. It is followed by tracking and explaining go-around data using the anomalous scores computed by TGP models.

Fig. 4 shows the mean and standard deviation (std) of S_x, for the medium and heavy categories when the aircraft vertically deviates from the glide slope. In general, velocity decreases as the aircraft approaches the touchdown point, which can be seen in S_x as it decreases along the glide slope from AKIPO to ABVON. For the

FID	Reported reasons for go-around. (WTC)	Anomaly in Z-scores $_{[D_a,D_b]}$
1	Pilot lost glide slope signal. (M)	$Z(P)\uparrow_{[7.60,0.50]}$, $Z(S_x)\uparrow_{[2.21,1.45]}$, $Z(S_y)\uparrow_{[1.92,0.89]}$, $Z(S_h)\updownarrow_{[2.43,0.50]}$
2	Pilot was unable to sight the landing runway. (M)	$Z(P)\uparrow_{[0.68,0.50]}$, $Z(S_x)\downarrow_{[2.90,2.58]}$, $Z(S_y)\downarrow_{[1.97,1.75]}$, $Z(S_h)\uparrow_{[2.90,2.76]}$
3	Tail wind of 21 knots and lost visual contact with the runway. (M)	$Z(S_y)\updownarrow_{[4.03,3.95]}$
4	Due to weather, unable to sight the runway. (M)	$Z(P)\uparrow_{[5.91,4.06]}$, $Z(S_x)\downarrow_{[4.78,4.23]}$, $Z(S_h)\uparrow_{[1.83,1.29]}$
5	Due to weather, unable to sight the runway. (M)	$Z(P)\uparrow_{[0.88,0.78]}$, $Z(S_x)\downarrow_{[0.85,0.71]}$, $Z(S_y)\downarrow_{[1.81,1.48]}$, $Z(S_h)\uparrow_{[1.01,0.64]}$
6	Due to poor visibility caused by heavy rain. (M)	$Z(S_y)\downarrow_{[4.38,4.33]}$, $Z(S_h)\updownarrow_{[4.19,2.98]}$
7	Due to wind sheer. (H)	$Z(P)\uparrow_{[3.52,3.51]}$, $Z(S_x)\uparrow_{[4.02,2.58]}$, $Z(S_y)\uparrow_{[1.23,1.18]}$, $Z(S_h)\downarrow_{[3.82,1.23]}$
8	Unstable approach due to "Floating". (H)	$Z(S_x)\downarrow_{[7.60,3.91]}$, $Z(S_h)\uparrow_{[6.29,5.34]}$
9	Due to wind sheer and poor visibilty. (H)	$Z(P)\uparrow_{[2.09,0.50]}$, $Z(S_x)\updownarrow_{[2.92,2.82]}$, $Z(S_y)\updownarrow_{[4.27,4.04]}$, $Z(S_h)\updownarrow_{[2.61,0.50]}$
10	Unstable approach. (M)	$Z(P)\uparrow_{[1.66,0.50]}$, $Z(S_x)\downarrow_{[4.18,3.53]}$, $Z(S_y)\uparrow_{[2.91,2.90]}$, $Z(S_h)\uparrow_{[2.16,0.50]}$
11	Unstable approach. (M)	$Z(S_x)\downarrow_{[5.11,3.85]}$, $Z(S_h)\uparrow_{[1.20,0.98]}$
12	Due to tail wind and high on approach. (M)	$Z(P)\uparrow_{[7.60,0.50]}$, $Z(S_x)\uparrow_{[7.44,3.15]}$, $Z(S_y)\downarrow_{[1.09,0.50]}$, $Z(S_h)\uparrow_{[5.86,0.50]}$
13	Unstable approach. (M)	$Z(P)\uparrow_{[2.61,2.30]}$, $Z(S_x)\downarrow_{[5.22,3.07]}$, $Z(S_y)\uparrow_{[3.30,2.93]}$, $Z(S_h)\uparrow_{[5.73,4.80]}$
14	Wind sheer and weather. (H)	$Z(P)\uparrow_{[1.64,0.50]}$, $Z(S_y)\downarrow_{[3.59,3.29]}$, $Z(S_h)\updownarrow_{[1.92,0.50]}$

TABLE I: Go-around dataset with anonymized flight ID (FID) and its associated anomalies tracked and explained by the proposed TGP model. Arrows indicate the sign of anomalous scores, $\uparrow,\downarrow,\updownarrow$ for positive, negative, and both, respectively. $[D_a, D_b]$ denotes the segment that has the longest consecutive anomalous scores along the glide slope, where D_a and D_b are the remaining distances to the runway threshold in nautical mile.

medium category, it is observed that deviation from above and below generally leads to higher speed and variation in speed. In contrast, the heavy category has greater fluctuation in speed when the aircraft deviates vertically below the glide slope. Overall, the std of S_x for the heavy category is generally lower than the medium category. This is due to the heavy category having greater weight and inertia. When aircraft laterally deviates from the localizer, greater variation in S_x and higher std of S_x are observed in Fig. 5.

Comparing supplementary Fig. S2 and S3, aircraft that deviate from ILS laterally have greater fluctuation in the mean of S_y and higher std. The std in both cases are generally decreasing along the glide slope, except for the aircraft with lateral deviation near ABVON. This can be due to interference in the A-SMGCS when the aircraft is getting closer to the runway. Supplementary Fig. S2 shows a fluctuation in the mean of S_y when the aircraft is located between 0.6 and 1.0 (normalized distance between AKIPO and ABVON). A positive peak is observed, followed by a negative deflection. This can be due to the artifact generated by the data fusion of A-SMGCS. Hence, the proposed TGP models probabilistically reveal this artifact. The mean of S_y in supplementary Fig. S3 is observed to deviate from zero from aircraft is deviated laterally from the center-line.

In supplementary Fig. S4, the mean of S_h is observed to be slower (less negative) when the aircraft is vertically below the glide slope and faster (more negative) when the aircraft is vertically above the glide slope. The std of S_h is mainly decreasing from AKIPO to ABVON. Supplementary Fig. S5 shows the descent rate when the aircraft laterally deviates from the localizer. It explains the difference between the circling approach (aircraft are being vectored to align with ILS) and the straight-in approach. The straight-in approach is observed to have a higher descent rate compared to the circling approach.

Subsequently, we select a few go-around flights with flight identity (FID) and provide the tracking visualization in Fig. 6-9. For evaluating the model's efficacy, TGP is applied on these trajectories to explain unstable approach parameters that lead to go-around, verified with METAR and go-around report. Based on the observation in the METAR and reports of go-around, it is found that weather and wind sheer made negative impacts on landing, which are also very well captured by the models. All the go-arounds are tabulated in Table I, and eight representative cases of go-arounds are discussed. The selected cases are visualized in Fig. 6-9. We showed the full 4D trajectories and color-coded progress bars of the associated TGP Z-scores. In real-time settings, the instantaneous anomalous Z-scores can be displayed using the streamed A-SMGCS data. A fast-time simulation of an approach and landing scenario is provided at https://simkuangoh.github.io/TunnelGP/Simulation/. The red markers are placed slightly below or above the normal (green) markers to indicate the signs of anomalous Z-scores.

Fig. 6 & 7 illustrate the 4D trajectories for FID $1, 12$ and the associated TGP Z-scores. FID 1 was reported to lose glide slope signal at 4.5 NM; thereby, no indication was available in the cockpit regarding correct landing

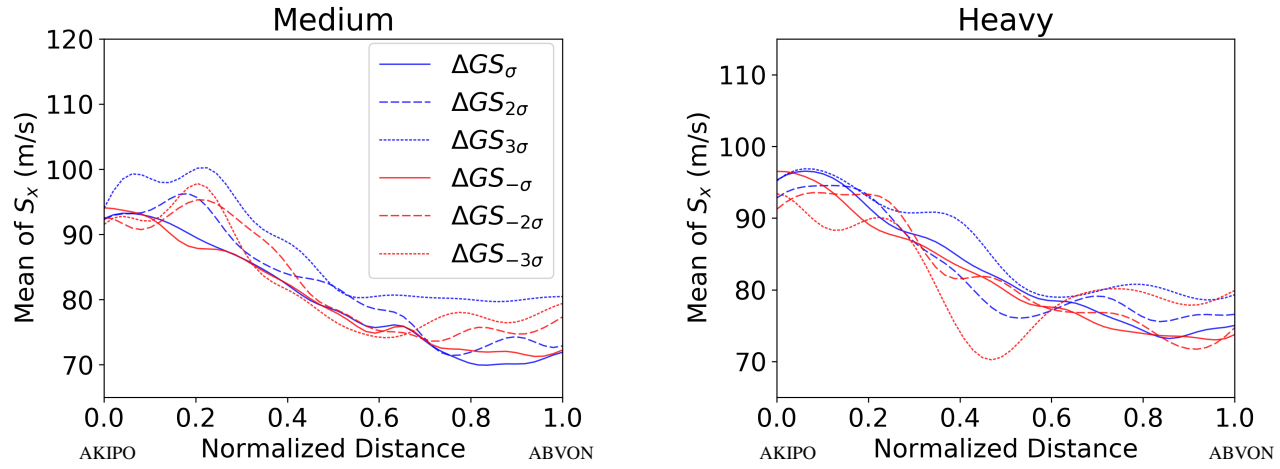

(a) Mean of S_x at different deviations $1\sigma, 2\sigma, 3\sigma$ from glide slope ΔGS, for medium (left) and heavy (right) categories. The figures show the influence of vertical deviation from glide slope to S_x.

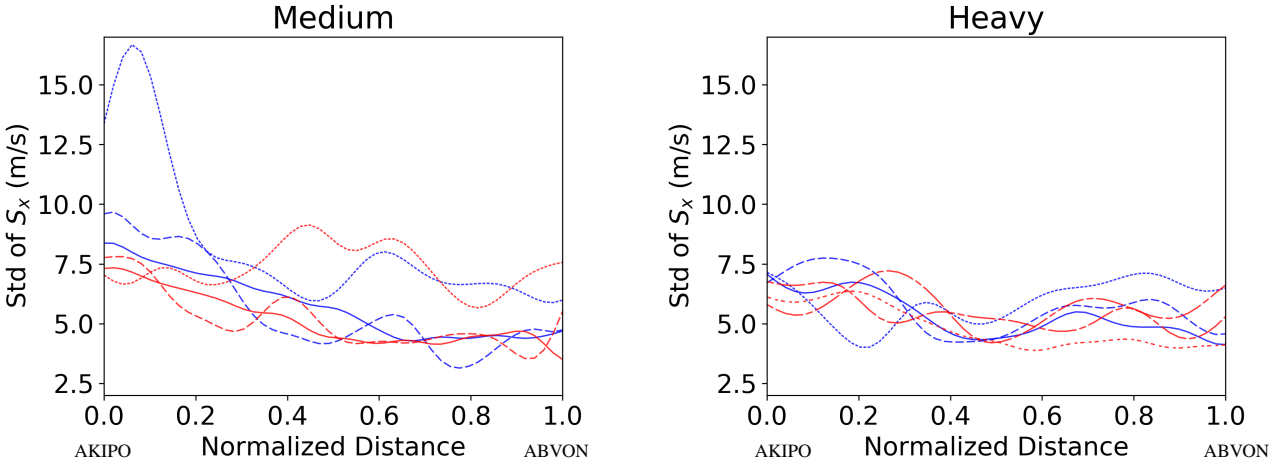

(b) Std of S_x at different deviations $1\sigma, 2\sigma, 3\sigma$ from glide slope ΔGS, for medium (left) and heavy (right) categories. The figures show the influence of vertical deviation from glide slope to S_x.

Fig. 4: The relationship between landing parameters S_x and vertical deviation along the normalized distance between AKIPO and ABVON.

parameters, which might have resulted in higher altitude and undesired speed leading to go-around. The associated Z-scores for FID 1 relate to the same findings. FID 12 also reported a tailwind along with being high on approach. When their associated TGP Z-scores are analyzed, $Z(P)$ were found to be anomalous all the way along the landing trajectories.

For FID 3 in Fig. 6, it is observed that anomalies detected were for a very small proportion of the flight track in lateral speed S_y, which suggests that the aircraft was flying in a stable configuration most of the time despite a very high tailwind component as reported. A correction was performed successfully to rectify the deviation in speed. However, the aircraft still performed a go-around not due to unstable approach parameters rather it was due to poor visibility (heavy rain reported in METAR during that time) and non-sighting of the runway as reported by the pilot.

In Fig. 7 & 8, the 4D trajectories for FID $13, 8$ and the associated TGP Z-scores are depicted. Visually, the 4D landing trajectory looks normal. The positional $Z(P)$ was normal for FID 8. However, $Z(P)$ was anomalous for a small period for FID 13. When the associated $Z(S_x), Z(S_h)$ are analyzed, TGP informs that the aircraft was flying too slow along the glide slope and descending at a slower rate compared to nominal flights. Both pilots reported unstable approaches, while FID 8 indicated ”floating”, which can be explained by their associated

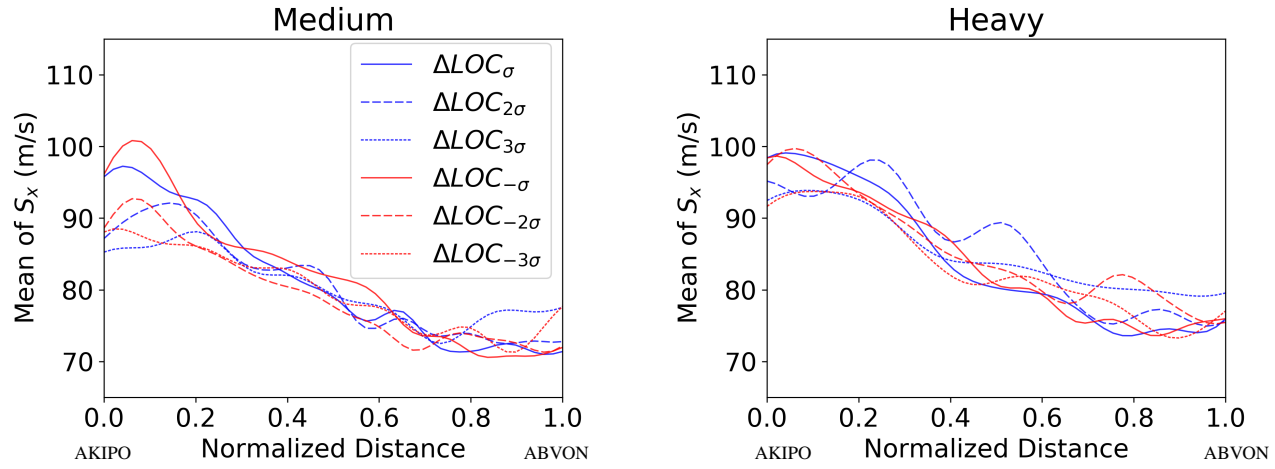

(a) Mean of S_x at different deviations $1\sigma, 2\sigma, 3\sigma$ from localizer ΔLOC, for medium (left) and heavy (right) categories. The figures show the influence of lateral deviation from localizer to S_x.

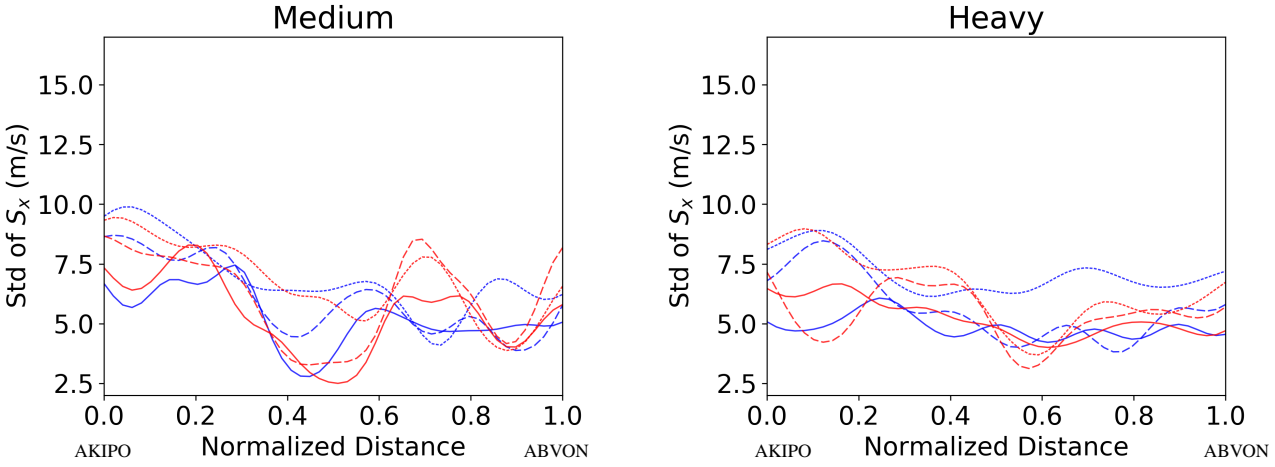

(b) Std of S_x at different deviations $1\sigma, 2\sigma, 3\sigma$ from localizer ΔLOC, for medium (left) and heavy (right) categories. The figures show the influence of lateral deviation from localizer to S_x.

Fig. 5: The relationship between landing parameters S_x and lateral deviation along the normalized distance between AKIPO and ABVON.

Z-scores. In contrast, FID 7 in Fig. 8 was flying too fast along the glide slope and had a greater descent rate compared to nominal flights, as indicated by TGP Z-scores. Wind shear was reported, and it can be the root cause of the anomaly in speed.

Wind shear was also reported to affect FID $9, 14$ in Fig. 9, while the pilot on FID 9 also reported poor visibility. Based on the Z-scores for speeds, we can postulate the location of wind sheer along the glide slope and how the wind sheer impacts the landing speeds S_x, S_y, S_h. Both aircraft performed a go-around before ABVON, and these are consistent with the $Z(P)$.

In summary, the proposed TGP models derive the interrelation between landing parameters. Besides, TGP explains how vertical and lateral ILS deviations lead to fluctuation in speed along different directions. Furthermore, we demonstrate how TGP can be utilized to track and explain the unstable approach parameters. TGP provides continuous spatio-temporal insights into landing parameters adherence. The proposed method can augment the existing stabilized approach and landing rules by providing a probabilistic description of a safe landing.

A. Comparison with mGMM

The results of mGMM are shown in Fig. 6-9, for a side-by-side comparison with TGP. The black markers indicate normal approaches, while the blue markers indicate

the signed anomalous events using triangular markers, pointing up for positive or down for negative values. Based on the results, several key observations are found:

1) TGP provides a continuous probabilistic description of normal versus anomalous events along the glide slope, while mGMM can only identify normal and anomalous events at selected discrete positions. No informed decision can be made when aircraft are flying in between the pre-selected positions.
2) The Z-Scores of mGMM have less consistency in anomalous event detection (signs are flipped abruptly, especially for $Z(S_h)$ in FID 7 and $Z(S_x), Z(S_y), Z(S_h)$ in FID 12), which wrongly indicates oscillating maneuver during the approach, while TGP provides a more consistent signed anomalous tracking and detection.
3) While some of the Z-scores by TGP match with mGMM, some of them contradict each other. For FID 1 and 13, aircraft with a high approach, both TGP and mGMM give the same $Z(P)$. However, mGMM is observed to have many false positives in $Z(P)$ and $Z(S_h)$ for many FIDs, which do not match with the reported reasons for go-around in Table I. Moreover, the tailwind was reported in FID 3, but mGMM failed to indicate an anomalous event in any speed $Z(S)$.

B. Potential Operational Scenarios

The interpretability of TGP can enable a few potential operational scenarios, where the software developers of air traffic management systems can customize indicators, triggers, and thresholds using comprehensible probabilistic descriptions of TGP to warn ATCO on the following events during the approach and landing:

- Aircraft is too high or low on the glide slope, but no correction attempt is observed.
- Aircraft has difficulty aligning with the localizer and deviates laterally from the runway center-line.
- Aircraft is flying at unintended speed.

For instance, an alarm can be triggered to warn ATCO if an anomalous event (e.g., too high on glide slope) occurred and lasted continuously for a certain amount of time or distance (e.g., from 4 NM to 3.7 NM from runway threshold) but no corrective actions (measured in terms of reducing anomalous scores) was taken over a certain amount of time or distance (e.g., 0.3 NM). In this case, the value $Z(P)$ will be larger than a threshold when the aircraft is at 4 NM to 3.7 NM from the runway threshold. The $Z(P)$ can be augmented with the P, to indicate the relative position of the aircraft relative to ILS. If $Z(P)$ violates the bound specified in Equation 8 for more than 0.3 NM, the values of P and $Z(P)$ can be presented to ATCO through an interface, together with other information, for example $Z(S_x)$, $Z(S_y)$, and $Z(S_h)$. If ATCO finds corrective action is necessary, an advisory call can be relayed to PIC. In the event that safety is compromised, ATCO can provide mandatory instruction for PIC to carry out a missed approach. The types and tolerance levels of warnings/alarms can be flexibly adjusted to account for the duration of the anomaly, the size and sign of the anomaly, as well as the corrective actions made by PIC. These can be periodically assessed and adjusted for customized sensitivity and specificity for different airport configurations and weather.

VI. CONCLUSION

The current study implements data-driven, probabilistic, and comprehensible TGP models to augment the existing rule-based stable approach criteria, by characterizing the 4D approach and landing parameters. As there is no ground truth and the exact borderline between normal and anomalous approach and landing parameters, we attempt the issues of unstable approach using data-driven TGP models on unlabelled approach and landing parameters. We show that the proposed TGP models can continuously elucidate the interrelation between approach and landing parameters and facilitate tracking and detection of unstable approach parameters. Moreover, TGP model was applied on go-around trajectories. Accordingly, the observed results suggest that TGP models are capable of detecting anomalous parameters during the approach path in all 14 go-around cases from 7.6 NM to 0.5 NM (missed approach point) away from the touchdown threshold and provide interpretable explanations and continuous insights of unstable approach along the glide slope. The comparative analysis of TGP with mGMM demonstrates several advantages (i.e., continuity, consistency, and comprehensibility) of the current study.

Currently, stabilized approach and decision to go-around are mainly managed by a pilot. The proposed interpretable TGP models can assist in the monitoring of safe landing to ATCO. Moreover, the adverse weather phenomenon in the approach path of aircraft, which causes violations of parameters, is also well captured by the TGP models. Hence, such models can enhance the situational awareness of ATCO and alert ATCO of anomalous landing events. Furthermore, ATCO can also communicate information about the violation of landing parameters to the pilot and can be involved in the decision-making of the go-around. This will facilitate ATCO to plan and re-sequence traffic ahead of time. Such TGP models can provide a ground-based safety net to the compliance of landing operations. Furthermore, such an unstable approach tracking method can be directly applied to other types of landing systems (e.g., GNSS Landing System and RNAV Approaches).

There are a few aspects of this work that can be extended to make an operational impact in real-time. Despite the unstable approach problem having been attempted in several works, it still lacks a comparative universal evaluation due to the difficulty of labeling the timing and stability in approach and landing parameters accurately in

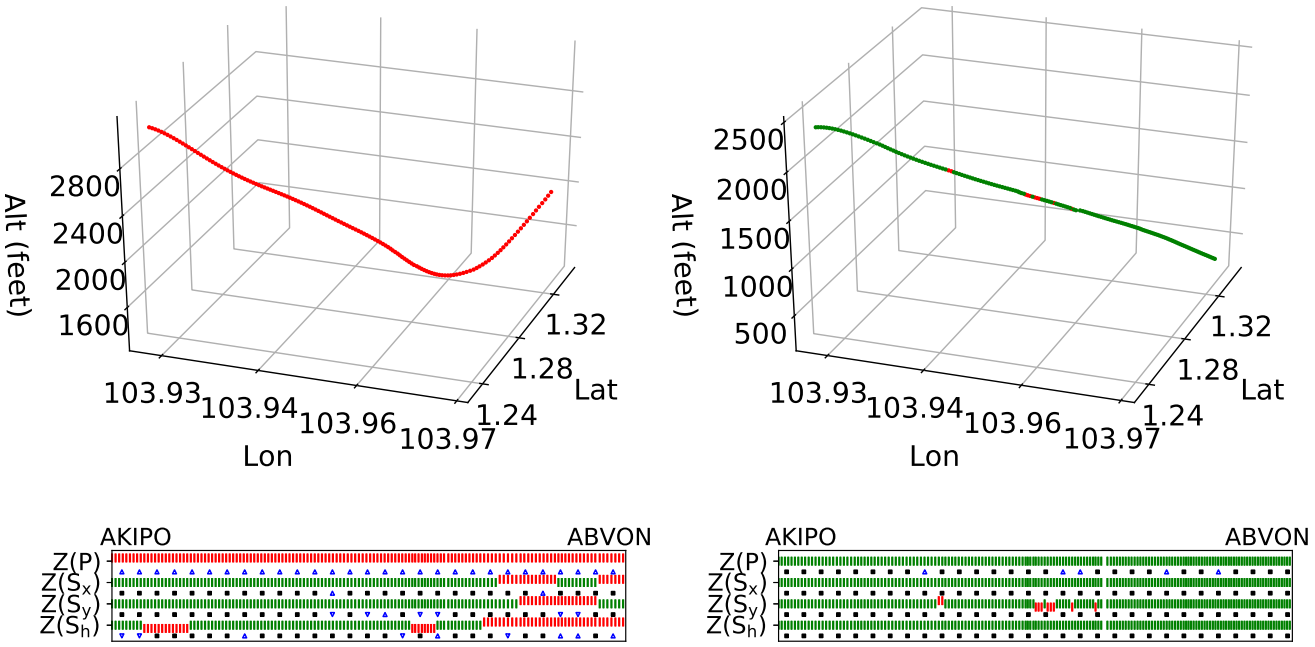

Fig. 6: 4D landing trajectories go-around cases (top) and the progress bars of associated Z-scores (bottom) for flights with identity FID 1 (left) and FID 3 (right) from Table I. The green (TGP) and black (mGMM) markers indicate normal approaches, while the signed red (TGP) and blue (mGMM) markers indicate anomalous events.

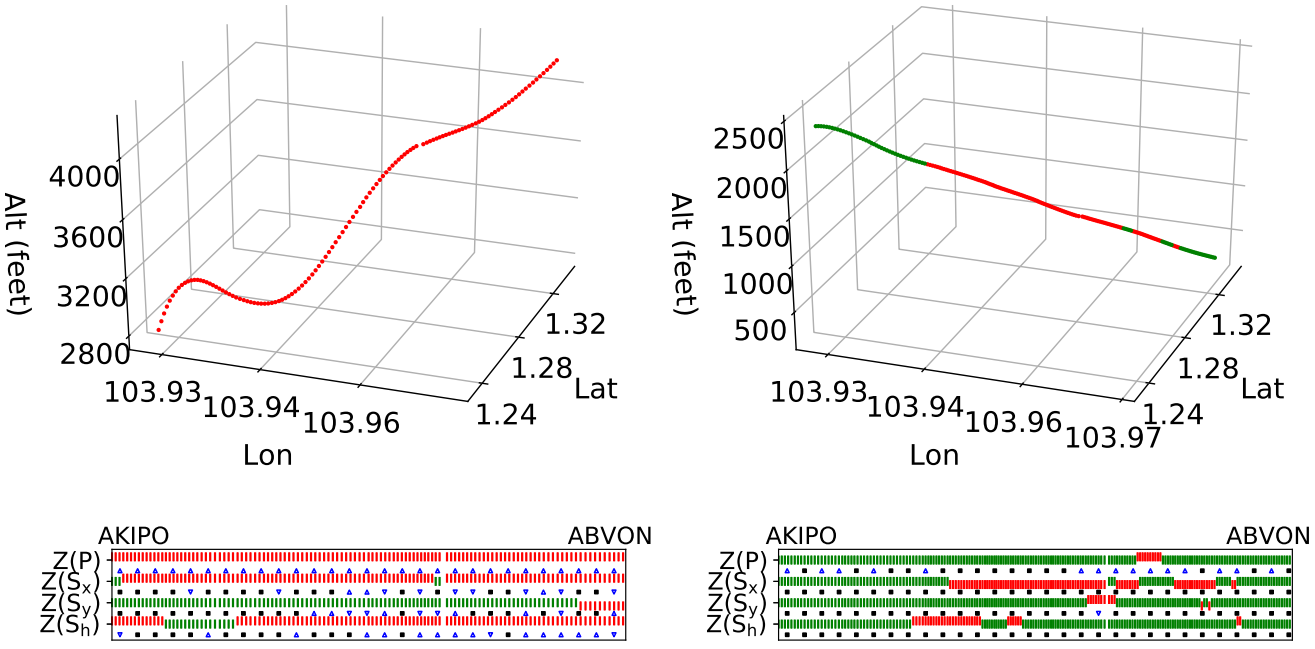

Fig. 7: 4D landing trajectories go-around cases (top) and the progress bars of associated Z-scores (bottom) for flights with identity FID 12 (left) and FID 13 (right) from Table I. The green (TGP) and black (mGMM) markers indicate normal approaches, while the signed red (TGP) and blue (mGMM) markers indicate anomalous events.

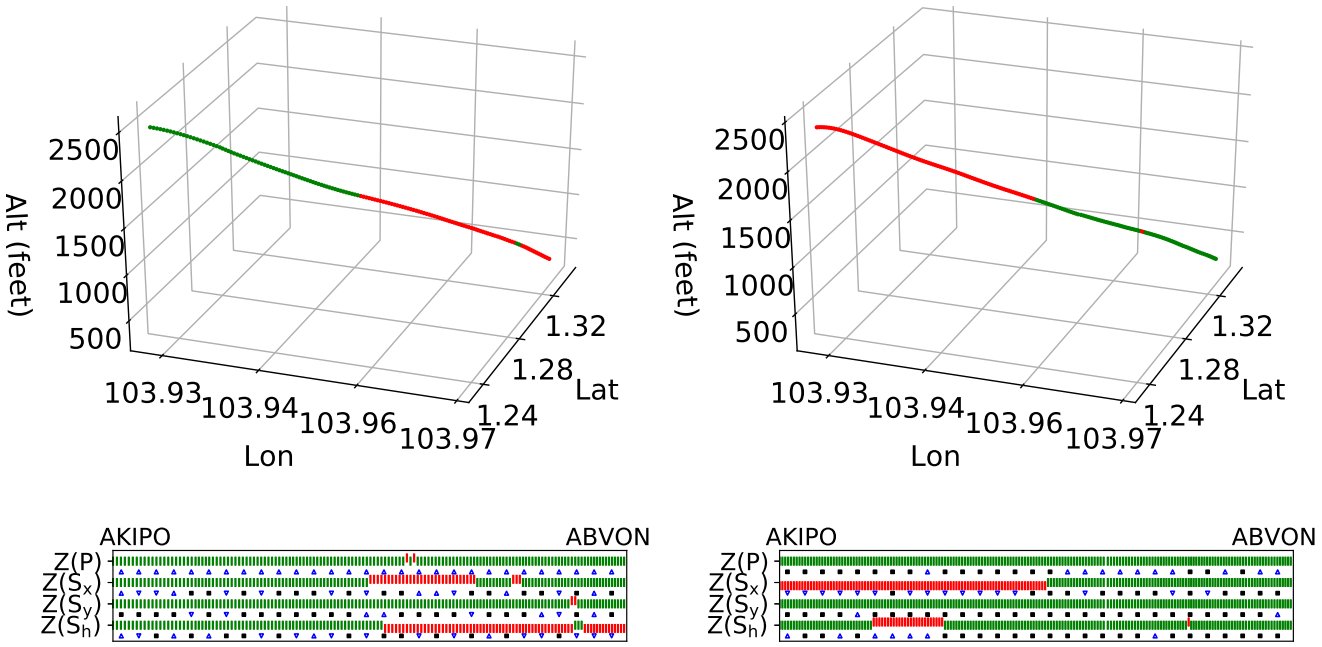

Fig. 8: 4D landing trajectories go-around cases (top) and the progress bars of associated TGP Z-scores (bottom) for flights with identity FID 7 (left) and FID 8 (right) from Table I. The green (TGP) and black (mGMM) markers indicate normal approaches, while the signed red (TGP) and blue (mGMM) markers indicate anomalous events.

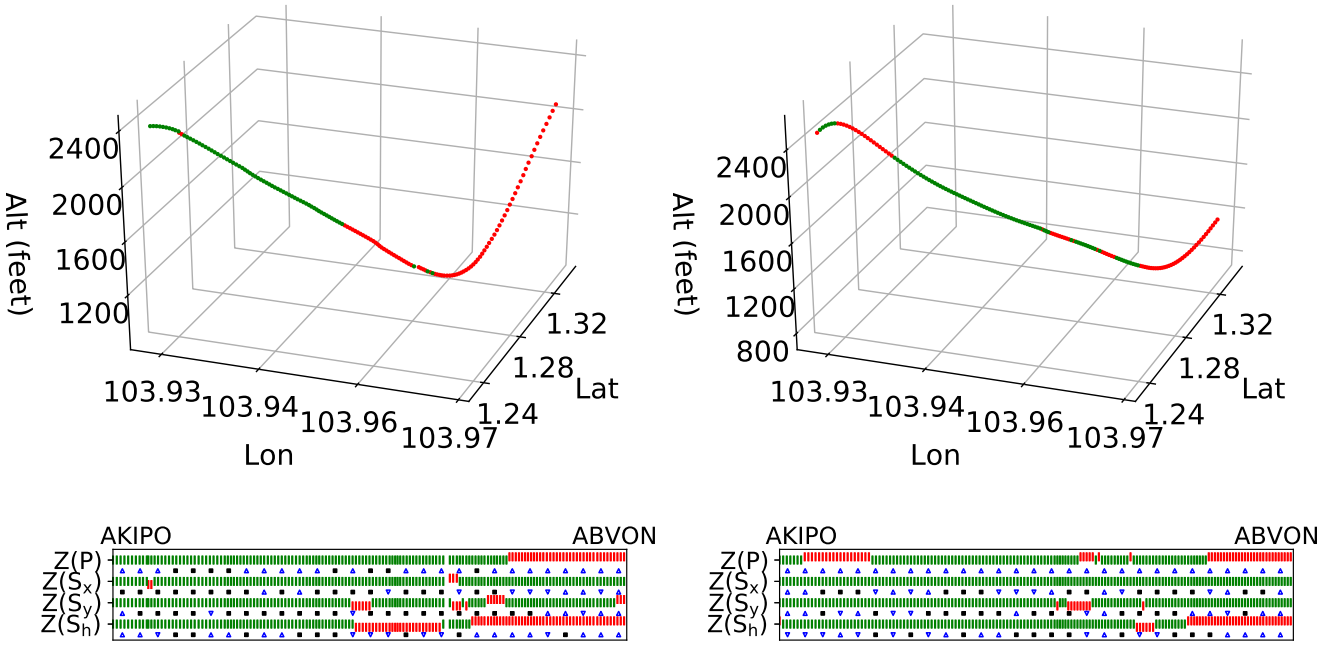

Fig. 9: 4D landing trajectories go-around cases (top) and the progress bars of associated TGP Z-scores (bottom) for flights with identity FID 9 (left) and FID 14 (right) from Table I. The green (TGP) and black (mGMM) markers indicate normal approaches, while the signed red (TGP) and blue (mGMM) markers indicate anomalous events.

practice. Future works that address this issue by developing a ground truth of timing and labels of (in)stability can facilitate a fair comparison between models and provide quantitative assessments of them. This work can be assessed in shadow mode, which provides a testbed using real air traffic data, as the proposed models are built around equipment already available in most airports (i.e., A-SMGCS and ILS).

REFERENCES

[1] International Air Transport Association (IATA)
Unstable approaches: risk mitigation policies, procedures and best practices. Montreal—Genevas: International Air Transport Association, 2016 2nd Edition.

[2] National Transportation Safety Board
(2019) Aviation safety alert 077: Stabilized approaches lead to safe landings. [Online]. Available: https://www.ntsb.gov/safety/safety-alerts/Documents/SA-077.pdf

[3] Boeing
Statistical summary of commercial jet airplane accidents: worldwide operations 1959–2016
Tech. Rep., 2019.

[4] International Air Transport Association (IATA)
(2019) Safety report. [Online]. Available: https://www.iata.org/en/publications/safety-report/

[5] Flight Safety Foundation
Go-around safety forum – findings and conclusions
Go-around Safety Forum Brussels, 2013.

[6] International Air Transport Association (IATA)
Operational safety audit (IOSA) standards manual. Montreal—Genevas: International Air Transport Association, 2016 11th Edition.

[7] FlightGlobal
(2013) Safety experts call attention to prevalence of unstable approaches. [Online]. Available: https://www.flightglobal.com/safety-experts-call-attention-to-prevalence-of-unstable-approaches/111538.article

[8] Civil Air Navigation Services Organization (CANSO)
Unstable Approaches. Civil Air Navigation Services Organisation, 2011, 2nd Edition.

[9] R. Casado, M. López-Lago, J. Serna, and A. Bermúdez
Enhanced missed approach procedure based on aircraft reinjection
IEEE Transactions on Aerospace and Electronic Systems, vol. 57, no. 6, pp. 4149–4170, 2021.

[10] S. K. Goh, N. P. Tran, D.-T. Pham, S. Alam, K. Izzetoglu, and V. Duong
Construction of air traffic controller's decision network using error-related potential
In *International Conference on Human-Computer Interaction*. Springer, 2019, pp. 384–393.

[11] J. Y. Zhong, S. K. Goh, C. J. Woo, and S. Alam
Impact of spatial orientation ability on air traffic conflict detection in a simulated free route airspace environment
Frontiers in human neuroscience, vol. 16, 2022.

[12] B. Ayhan, C. Kwan, Y.-B. Um, B. Budavari, and J. Larkin
Semi-automated emergency landing site selection approach for uavs
IEEE Transactions on Aerospace and Electronic Systems, vol. 55, no. 4, pp. 1892–1906, 2018.

[13] S. K. Goh, Z. Jun Lim, S. Alam, and N. Pratap Singh
Tunnel gaussian process model for learning interpretable flight's landing parameters
Journal of Guidance, Control, and Dynamics, pp. 1–12, 2021.

[14] J. Hegde and B. Rokseth
Applications of machine learning methods for engineering risk assessment – a review
Safety Science, vol. 122, p. 104492, 2020.

[15] J. Sun, H. A. Blom, J. Ellerbroek, and J. M. Hoekstra
Particle filter for aircraft mass estimation and uncertainty modeling
Transportation Research Part C: Emerging Technologies, vol. 105, pp. 145–162, 2019.

[16] S. K. Goh, H. A. Abbass, K. C. Tan, A. Al-Mamun, C. Wang, and C. Guan
Automatic eeg artifact removal techniques by detecting influential independent components
IEEE transactions on emerging topics in computational intelligence, vol. 1, no. 4, pp. 270–279, 2017.

[17] S. Wang, W. Liu, J. Wu, L. Cao, Q. Meng, and P. J. Kennedy
Training deep neural networks on imbalanced data sets
In *2016 international joint conference on neural networks (IJCNN)*. IEEE, 2016, pp. 4368–4374.

[18] S. Hosseini and H. Seilani
Anomaly process detection using negative selection algorithm and classification techniques
Evolving Systems, pp. 1–10, 2019.

[19] B. Krawczyk, M. Galar, M. Woźniak, H. Bustince, and F. Herrera
Dynamic ensemble selection for multi-class classification with one-class classifiers
Pattern Recognition, vol. 83, pp. 34–51, 2018.

[20] T. Amarbayasgalan, B. Jargalsaikhan, and K. H. Ryu
Unsupervised novelty detection using deep autoencoders with density based clustering
Applied Sciences, vol. 8, no. 9, p. 1468, 2018.

[21] J. Fan, Q. Zhang, J. Zhu, M. Zhang, Z. Yang, and H. Cao
Robust deep auto-encoding gaussian process regression for unsupervised anomaly detection
Neurocomputing, vol. 376, pp. 180–190, 2020.

[22] L. Dai, Y. Liu, and M. Hansen
Modeling go-around occurrence
presented at the Thirteenth USA/Europe Air Traffic Management Research and Development Seminar (ATM, vol. 2019, 2019.

[23] N. P. Singh, S. K. Goh, and S. Alam
Real-time unstable approach detection using sparse variational gaussian process
In *2020 IEEE International Conference on Artificial Intelligence and Data Analytics for Air Transportation (AIDA-AT)*, 2020, pp. 1–10.

[24] R. J. de Boer, T. Coumou, A. Hunink, and T. van Bennekom
The automatic identification of unstable approaches from flight data
In *6th International Conference on Research in Air Transportation, ICRAT*, 2014, pp. 26–30.

[25] L. Sherry and J. Shortle
Improving the nowcast of unstable approaches
8th International Conference on Research in Air Transportation, 2016.

[26] T. Puranik, N. Rodriguez, and D. Mavris
Towards online prediction of safety-critical landing metrics in aviation using supervised machine learning
Transportation Research Part C: Emerging Technologies, vol. 120, 2020.

[27] L. Li, R. J. Hansman, R. Palacios, and R. Welsch
Anomaly detection via a gaussian mixture model for flight operation and safety monitoring
Transportation Research Part C: Emerging Technologies, vol. 64, pp. 45 – 57, 2016.

[28] J. Baek and H. Balakrishnan
A game-theoretic analysis of reallocation mechanisms for airport landing slots
IEEE Transactions on Intelligent Transportation Systems, pp. 1–14, 2019.

[29] M. Niendorf, P. T. Kabamba, and A. R. Girard
Stability analysis of runway schedules
IEEE Transactions on Intelligent Transportation Systems, vol. 17, no. 12, pp. 3380–3390, 2016.

[30] S. T. Barratt, M. J. Kochenderfer, and S. P. Boyd
Learning probabilistic trajectory models of aircraft in terminal airspace from position data
IEEE Transactions on Intelligent Transportation Systems, vol. 20, no. 9, pp. 3536–3545, 2018.
[31] W. J. Eerland, S. Box, H. Fangohr, and A. Sóbester
A gaussian process based decision support tool for air traffic management
In *17th AIAA Aviation Technology, Integration, and Operations Conference*, 2017, p. 4264.
[32] G. Chatterji
Short-term trajectory prediction methods
In *Guidance, Navigation, and Control Conference and Exhibit*, 1999, p. 4233.
[33] G. Chatterji, B. Sridhar, and K. Bilimoria
En-route flight trajectory prediction for conflict avoidance and traffic management
In *Guidance, Navigation, and Control Conference*, 1996, p. 3766.
[34] M. Gariel, A. N. Srivastava, and E. Feron
Trajectory clustering and an application to airspace monitoring
IEEE Transactions on Intelligent Transportation Systems, vol. 12, no. 4, pp. 1511–1524, 2011.
[35] L. Li, R. J. Hansman, R. Palacios, and R. Welsch
Anomaly detection via a gaussian mixture model for flight operation and safety monitoring
Transportation Research Part C: Emerging Technologies, vol. 64, pp. 45–57, 2016.
[36] S. K. Goh, H. A. Abbass, K. C. Tan, A. Al-Mamun, C. Guan, and C. C. Wang
Multiway analysis of eeg artifacts based on block term decomposition
In *2016 International Joint Conference on Neural Networks (IJCNN)*. IEEE, 2016, pp. 913–920.
[37] S. K. Goh *et al.*
Spatio–spectral representation learning for electroencephalographic gait-pattern classification
IEEE Transactions on Neural Systems and Rehabilitation Engineering, vol. 26, no. 9, pp. 1858–1867, 2018.
[38] M. A. Ahmad, C. Eckert, and A. Teredesai
Interpretable machine learning in healthcare
In *Proceedings of the 2018 ACM international conference on bioinformatics, computational biology, and health informatics*, 2018, pp. 559–560.
[39] J. Sipple
Interpretable, multidimensional, multimodal anomaly detection with negative sampling for detection of device failure
In *International Conference on Machine Learning*. PMLR, 2020, pp. 9016–9025.
[40] M. Du, N. Liu, and X. Hu
Techniques for interpretable machine learning
Communications of the ACM, vol. 63, no. 1, pp. 68–77, 2019.
[41] A. Boopathy *et al.*
Proper network interpretability helps adversarial robustness in classification
In *International Conference on Machine Learning*. PMLR, 2020, pp. 1014–1023.
[42] Z. J. Lim, S. K. Goh, I. Dhief, and S. Alam
Causal effects of landing parameters on runway occupancy time using causal machine learning models
In *2020 IEEE Symposium Series on Computational Intelligence (SSCI)*. IEEE, 2020, pp. 2713–2722.
[43] L. Rieger, C. Singh, W. Murdoch, and B. Yu
Interpretations are useful: penalizing explanations to align neural networks with prior knowledge
In *International Conference on Machine Learning*. PMLR, 2020, pp. 8116–8126.
[44] J. Hensman, A. Matthews, and Z. Ghahramani
Scalable variational gaussian process classification
2015.
[45] E. Padonou and O. Roustant
Polar gaussian processes and experimental designs in circular domains
SIAM/ASA Journal on Uncertainty Quantification, vol. 4, no. 1, pp. 1014–1033, 2016.
[46] E. Piazza
A-smgcs routing and guidance functions
IEEE Aerospace and Electronic Systems Magazine, vol. 15, no. 7, pp. 15–23, 2000.
[47] Z. Ghahramani and G. E. Hinton
Parameter estimation for linear dynamical systems
Technical Report CRG-TR-96-2, University of Totronto, Dept. of Computer Science, Tech. Rep., 1996.
[48] D. P. Kingma and J. Ba
Adam: A method for stochastic optimization
arXiv preprint arXiv:1412.6980, 2014.

Sim Kuan Goh (Senior Member, IEEE), obtained his B. Eng. and Ph.D. from the National University of Singapore in 2013 and 2019. He is currently an assistant professor at Xiamen University, Malaysia. Prior to joining Xiamen University Malaysia, he was a research fellow at the Air Traffic Management Research Institute, Nanyang Technological University. His research focuses on computational intelligence and its applications.

Narendra Pratap Singh received Master's degree in Computer Science from Jawaharlal Nehru University in 2002. He is currently working as Assistant General Manager (ATM) and Associate Member (R&D) at the Airports Authority of India, Lucknow. His research areas include optimization algorithms in air traffic management and innovation.

Zhi Jun Lim received the B.Eng degree in Aerospace Engineering and B.A degree in Economics from Nanyang Technological University, Singapore, in 2019. She is currently pursuing the Ph.D. degree with the Air Traffic Management Research Institute, Nanyang Technological University, Singapore. Her research work focuses on machine learning and artificial intelligence with applications in air traffic management.

Sameer Alam is Associate Professor at the School of Mechanical and Aerospace Engineering, NTU. He received Ph.D. degree (2008) in Computer Science with specialization in Artificial Intelligence from University of New South Wales (UNSW) Australia. He is the Deputy Director of ATMRI, NTU. He is also the editorial board member of Transportation Research Part-C. His research interests are in Machine Learning, Computer Vision, Multi-Agent Systems, applied to Air Traffic and Airport operations.